Influence of Thermal Ageing on the Electrochemical Corrosion Behaviour of Al-3.5% Cu-0.8% Mg/DOUM Palm Nut Shell Ash Particulate (DPNSAp) Composite

MAHDI SANI UDU[1], AUWAL KASIM[2], UMAR SHEHU[3], EVARASTICS POLYCARP[4]

[1, 4] *Department of Metallurgical Engineering Technology, WaziriUmaru Federal Polytechnic, Birnin Kebbi.*

[1, 2, 3] *Department of Metallurgical and Materials Engineering, Ahmadu Bello University, Zaria.*

Abstract- The influence of thermal ageing on the electrochemical corrosion behavior of Al-3.5%Cu-0.8%Mg/Doum Palm Nut Shell Ash particulate (DPNSAp) composite was investigated. DPNSAp reinforcement was characterized using Zetasizer Analyser and X-Ray Diffractometer (XRD). The composite was developed via the stir casting method by incorporating 3.0, 6.0 and 9.0wt% (DPNSAp) reinforcement with the base alloy as control. Solution heat treatment was carried out on the developed samples and corrosion examinations were carried out using Linear Polarization Resistance (LPR) method. Morphological examination was carried out on the as-cast and aged samples using a Scanning Electron Microscope (SEM). The results obtained from Zetasizer Analyzer showed that the reinforcement had an average particle size of 639.6 nm, and a Poly Dispersion Index (PDI) of 0.595 which is an indication of wide variation in particle sizes. Additionally, characterization of the reinforcement by (XRD) revealed the presence of 41% Quartz (SiO_2), 44% Albite ($Na.Al.Si_3.O_8$), 4.2% Muscovite ($H_2.K.Al_3.(SiO4)_3$), 6.9% Orthoclase ($Al_2O_3.K_2O.6SiO_2$), 0.013% Chlorite ($Al-Fe-SiO_2-O$) and 4.1% Sylvite (KCl). Linear Polarization Resistance (LPR) of the as-cast and aged samples showed a decrease in the corrosion rate from 4.15 to 1.11 mils/year for the control sample and 1.87 to 1.39 mils/year for the 9% reinforced sample. Morphological examination of the base alloy showed pits and craters with $CuAl_2$ intermetallics within the Al-Matrix which after exposure to artificial seawater showed localized corrosion along grain boundaries. The morphology of the reinforced samples showed reinforcement particles agglomerating along grain boundaries and cracks in the matrix which upon ageing were dispersed within the matrix.

Indexed Terms- Aluminium Composite, Doum Palm, Stir casting, LPR, Electrochemical corrosion.

I. INTRODUCTION

Composite materials, plastics and ceramics have been the dominant emerging materials in many industries over the last decade. The motive behind the use of Metal Matrix Composite (MMCs) components in the automotive, agriculture and mining sectors is based on requirements for weight reduction and, the pursuit of high-efficiency and performance materials. The automotive industry is subjected to increasingly strict fuel economy requirements by consumers demanding improved comfort and safety. To meet these requirements, automotive manufacturers are turning to lightweight and improved efficient products. The possibility of taking advantage of particular properties of the constituent materials to meet specific demands is the most important motivation for the development of composites[1].

A composite is a material that is produced via a physical combination of pre-existing constituent materials to obtain a new material with unique properties when compared to monolithic materials. The term"matrix", as often used in composite materials, refers to the percolating "soft" phase (which has generally excellent ductility, formability and thermal conductivity) in which are embedded the hard"reinforcements" (high stiffness and low thermal expansion). The reinforcements can be continuous or discontinuous, orientated or disorientated[1].

Metal-Matrix Composites (MMCs) have emerged as a class of materials capable of being utilized in advanced structural, aerospace, automotive, electronic, thermal management and wear applications. The performance advantage of Metal Matrix Composites is in their tailored mechanical, physical and thermal properties, high thermal conductivity, high abrasion and wear resistance[1]. The ever-increasing demand for low-cost reinforcement stimulated the interest towards the production and utilization of by-products from the industry as reinforcements since they are readily available at an affordable cost[2].

Age hardening is an important process that enhance the properties of metals. It is considered to be a novel way to increase the strength of the Aluminum alloys which are used for aerospace, marine, automotive and other engineering applications. Aluminum alloy 2024 (AA2024) is one such alloy which is often used for these applications and therefore, the study of its age hardening has been a prime topic of research. It is well accepted that the microstructure of the aged AA2024 consists of Guinier–Preston–Bagaryatsky (GPB) zones that are formed during the initial stages of the ageing treatment and are coherent with the matrix. With the increase in ageing temperature, these transform into the metastable Al_2CuMg ($¢S$) and Al_2Cu ($¢Q$) precipitates which act as precursors of the equilibrium S and Q phase intermetallic particles. The structure of $¢S$ and $¢Q$ has been found similar to S and Q precipitates with only a small difference in their lattice parameters. Various studies were conducted on the understanding of the formation and role of these precipitates on the hardness and strength of the aged Al–Cu–Mg alloys. The literature shows that the hardening of the aged Al–Cu–Mg alloys depends upon the distribution and types of these precipitates in the matrix. The formation of S-phase precipitates in Al–Cu–Mg alloys during the ageing treatment is found to be more useful in increasing the hardness and strength of the alloy than the Q-phase precipitates [3].

One of the important properties that is required of composite materials and other metals is the corrosion properties. Corrosion of metals could weaken the metal thereby reducing its lifespan during service and may cause failure of machines, building and other structure that could lead to loss of lives. The focus of this paper therefore, is to investigate the effect of electrochemical corrosion of Al-3.5%Cu-0.8%Mg/Doum Palm Nut Shell Ash particulate (DPNSAp) composite in seawater and to observe the morphology of the corroded surface using SEM.

II.   LITERATURE REVIEW

1. The electrochemical and corrosion properties of intermetallic particles in 2xxx Aluminium alloy were analysed by researchers devoted to the examination of the electrochemical properties of Al_2CuMg intermetallic particles (the S phase). These particles, due to the selective dissolution of Mg and Al, become enriched in copper and thus extremely cathodic. Al_2Cu particles are present in a substantially smaller amount than Al_2CuMg particles. These particles are highly cathodic compared with the solid solution of Aluminium 2xxx alloy. Clusters of Al_2Cu and Al2CuMg particles are the most common sites of localized corrosion.[4]

2. The effect of double thermal ageing treatment (DTAT) on the hardness, impact and tensile properties of Al-Cu-Mg/rice husk ash composite produced by the double stir casting method has been studied. From the results obtained, DTAT samples showed better hardness, impact and tensile properties as compared with the STAT samples. These significant improvements were evidenced in the DTAT for 5 h (with a hardness value of 81.3 HRB) and DTAT for 4 h with an impact strength of 72 kJ/m2 and Ultimate tensile strength of 129.797 N/mm2 respectively. The microstructural analysis revealed that more precipitates were formed and more evenly distributed in the DTAT than in STAT. It can be deduced that the thermal treatment has improved the mechanical properties of the composite studied under this condition [5].

3. The erosion–corrosion behavior of AA5052 aluminium alloy was studied in 3.5 wt% NaCl solution containing silica sand as an erodent particle. The tests were carried out according to ASTM G119-09 standard using a slurry jet apparatus at a jet velocity of 3 m/s, sand concentration of 90 g/l, and various impingement angles of 25°–90°. The pure erosion rates were

also obtained using cathodic protection of the samples during erosion–correction tests. Results showed that maximum pure erosion and erosion–corrosion rates occurred at an impingement angle of 30°. On the other hand, a negative synergism rate was obtained under all conditions tested. Energy dispersive spectrometry analysis suggested that the negative synergism could be attributed to the existence of a protective oxide layer formed on the eroded surface of the samples during erosion–correction tests [6].

4. Dynamic Mechanical analysis (DMA) was conducted on Doum palm shell particles reinforced polypropylene composite. Effects of Doum palm shell particle loading and temperature on the dynamic mechanical properties of the composites were studied. The results showed that Doum palm shell particles had a positive effect on the moduli and damping factor of the composites. The storage and loss modulus of the composite decreases with an increase in temperature while tan δ increases as the temperature increases. The study indicates that the increased modulus is attributed to the physical interaction between the polymer and Doum palm Shell particles that restrict the segmental mobility of the polymer chains. The increase in damping factor with temperature showed no significant effect on particle loading.[7]

5. Research was conducted to calculate the Corrosion Penetration Rate (CPR) of Aluminum matrix composite materials (AlSi10Mg (b)) with Silicon carbide (SiC*) reinforcement with the variation of matrix composite percentage. A wet corrosion test was conducted by dipping AlSi10Mg(b) and AlSi10Mg(b)+SiC* in the solution of HCl acid, NaOH, NaCl. The wet corrosion tests were also being done in the different pH (1,3,5,7,9,11, and 13). It was found that the highest corrosion penetration rate occurred when the specimen dipped in HCl solution when the pH was 1. We also observed that the addition of SiC* could reduce the corrosion rate of materials. Finally, this study showed that composite material, AC-43100 (AlSi10Mg (b)) 85% + 15% SiC*, has the best corrosion resistance [8].

6. The synergistic inhibition effect of Ce4+ and Melamine (M) on the corrosion of Aluminium alloy 2024 (AA2024) in 3.5% NaCl solution was investigated. Potentiodynamic Polarization (PDP) and Electrochemical Impedance Spectroscopy (EIS) techniques were used to study the synergistic effect of different Ce4+/M ratios on the corrosion behaviour of AA2024. The PDP study showed that a combination of 50% Ce4+ and 50% M leads to the lowest corrosion rates, both acting as cathodic inhibitors. Both PDP and EIS results indicated that M or Ce4+ in isolation did not offer effective corrosion protection, while the combination of M and Ce4+ significantly enhanced the corrosion protection with a synergism parameter equal to 3.5. SEM and EDX observations confirm the findings from the electrochemical techniques. XPS was used to investigate the mechanism of protection, revealing that the reduction of Ce4+ to Ce3+ occurs during the protection of AA2024. A new mechanism of corrosion synergistic inhibition by Ce4+ and organic compounds is postulated where the role of the organic compounds is to enhance the reduction of Ce4+.[9]

7. Abbass, Hassan and Alwan[10] studied the corrosion resistance of a metal matrix composite of an aluminum alloy (Al 6061) reinforced by SiC particles with 10wt% and 20wt%. Composite materials were prepared by stir casting using vortex technique. Corrosion behavior of aluminum matrix composite in seawater (3.5% NaCl solution) was examined using potentiostatically polarization measurements. The corrosion rate was calculated by Tafel equation and from the achieved polarization results. It was found that adding of SiC particles to the aluminum alloy matrix increases the corrosion rate. It was shown that the corrosion resistance decreases with increasing of SiC particles as compared to base alloy.

III.   MATERIALS AND METHODS

The materials and methods used in this research are discussed in subsequent sections

a) Materials

The materials used consist of pure Aluminium and copper wires which were obtained from Northern Cable Company (NOCACO) in Kaduna, Magnesium was purchased from a Chemical Vendor, while Doum palm nut shells were obtained from Birnin Kebbi market. Other materials used such as acetic acid, sulphuric acid, nitric acid, methanol, polishing powder, Bakelite, Grit papers, Acetone, Araldite, Benzene and sodium chloride were purchased over-shelf. Moulding sand and mould boxes were also used.

b) Equipment

The equipment used for this research work includes the following: Zetasizer Analyzer version 7.01, Potentiostat Galvanometer, X-Ray Diffractometer LR 39487C, Scanning Electron Microscope ZeisEvo LS10, digital weighing machine, X-Ray FluorescenceNTF-120A, Electrical resistance Furnace, Universal Testing Machine, ball mill, polishing machine, and Grinding machine.

c) Methods

This section shows the methods that were followed to produce the samples and carry out the mechanical and corrosion tests.

• Preparation of solution for corrosion testing

The solution used for the corrosion tests is artificial sea water which was prepared using 1000 ml distilled water with 35 g of NaCl at room temperature.

• Preparation of the Doum Palm Nut Shell Ash particulates (DPNSAp)

Doum Palm Nut shells recovered from the waste dumps were dried using hot air in roasters, pulverized and heated in a Furnace for 4 hours at a temperature of about 1200^oC with limited air till all volatile carbonaceous materials were completely burned. The resulting ash was ground in a Retsch Planery Ball Mill PM 400 with jars eccentrically arranged in its sun wheel. The movement of the sun wheel opposite to its grinding jars was at 1:2 (1:2.5 or 1:3) for 2, 4, 6, 8, and 10 hours at 300rpm with ball to powder ratio of 10:1.

• Particle size analysis of the DPNSAp

Particle size analysis was carried out using the Zetasizer Analyzer(version 7.01).

0.05mg of the sample was poured into a jar of distilled water. The Analyzer employed Dynamic Light Scattering (DLS) to measure the Brownian motion of particles placed in the holder by a laser light which analyzed the particle size distribution and generated a curve after multiple measurements. The Zetasizer software provided the average particle size (z-average), size distribution and Poly Diversity Index (PDI).

• X-ray diffraction (XRD)

X-ray diffraction of the DPNSAp sample was carried out using an "X"PertProP ANanalytical, LR 39487C XRD diffractometer using CuKά (ά=1.5148Å) at a34kV and a current of 25mA in a 2Θangular range between 10-90° every 0.04^o for 6s'. The sample was aligned in the equipment and the scan was initiated at several angles where the X-rays hit the crystal lattice to undergo constructive interference which led to diffraction. The intensity of the diffracted rays and the angles were recorded. The phases present were identified using the in-built software which matched the diffraction pattern to the crystal structure database.

• Production of Al-3.5%Cu-0.8%Mg/Doum Palm Nut Shell Ash particulate composite

The composite used in this study was Al-3.5%Cu-0.8%Mg/DPNAp composite containing 3–9wt% DPNSA particles at 3%wt intervals. Aigbodion and Hassan[11] produced aluminium composite samples using the Stir-Casting method. Pure Aluminium was added into the graphite crucible and heated to about 700^oC until the metal was completely fluid followed by the addition of Ligand (3.5g/1000g of Aluminium) and Magnesium (0.8g/1000g of Aluminium) into the molten metal. Additionally, the liquid melt was stirred for about 2 minutes until it was thoroughly mixed. 3wt% of DPNSAp was added to the developed alloy and the resulting composite was superheated to about 750^oC and stirred before being poured into a preheated sand mould to form cast samples with dimensions 15 x 300mm and 25 x 50 x 6 mm for cylindrical and rectangular bars respectively.

d) Solution Heat Treatment and age-hardening

Solution heat treatment was carried out on 39 samples in a Searchtech resistance furnace model SX-5-12. The samples were heated in the furnace to 490°C for 1 hour to obtain a homogenized uniform structure. A supersaturated solid solution (SSSS) was produced by quenching in cold water then artificial ageing was carried out at 190°C for 8 hours in the furnace. A schematic representation of the process is shown in Figure 1.
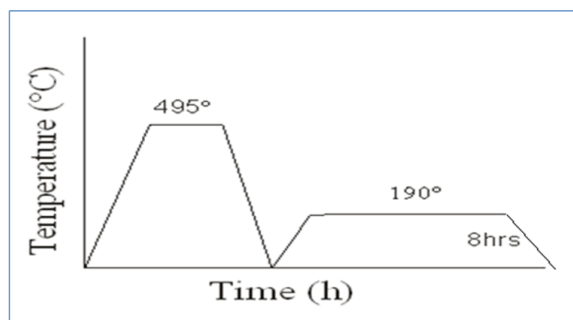

Figure 1: Schematic representation of the ageing treatment procedure of the composite

e) Corrosion test

• Sample preparation

A total of 5 coupons (one for each composition) for the test were machined to 10 x 15mm and then attached to a copper wire using epoxy mounting resin (Araldite) with connecting wire insulated from the solution and extending into the mounting to give a flat disc surface for contact with the solution. The samples were micro-polished using a digital polishing machine (Struers TegraPOL11!/Tegra Doser-5) in a Dia Duo suspension of different grades to achieve a mirror-like finish. The coupons were immersed in boiling Benzene for 5 minutes, removed and cleaned before finally being dried in a dessicator by the ASTM-G59-97 standard.

• Test procedure

Potentiodynamic polarization was conducted in an Autolab 302N Potentiostat with General Purpose Electrochemical Software (GPES). This equipment allows resolutions of 0.76 μV and 10nA for current signals respectively. Potentiodynamic polarization was conducted in a conventional three-electrode cell. A platinum rod was used as the counter and a saturated (KCl) Ag/AgCl electrode as a reference electrode. The samples were immersed in the solution before potentiodynamic polarization measurements and Polarization curves were recorded at a scan rate of 1 mV/s and GPES software was used for the determination of corrosion current densities and other polarization parameters.

• Surface Characterization using Scanning Electron Microscopy (SEM)

A total of 8 coupons were cleaned with isopropyl alcohol, dried in a desiccator and mounted on an epoxy resin. The material was coated with Gold to improve image quality before placing it in a Scanning Electron Microscope (Model: JSM-IT710HR). Their surface morphologies were studied by focusing electron beams with high-energy Electrons which interact with the samples to produce signals. The sample surfaces emit secondary electrons which provide topographical information used to produce imaging in association with the backscattered electrons. This resulted in generating high-resolution images of the sample surfaces thereby revealing the morphology of the samples at magnifications of 100, 200 and 500μm.

IV.   RESULTS AND DISCUSSION

The results obtained in the course of this study are hereby presented and discussed in this section.

a. Particle size analysis

Figure 2 shows the distribution of the particles according to the volume with peak values of 243.1nm and 482.1nm with 34.7 and 65.3% volume respectively. Similarly, Figure 3 shows peak sizes of 242.2nm and 4369nm with 55.4 and 44.6% intensity respectively while the average (z-average) particle size of 639.6nm was obtained. The Poly Dispersion Index (PDI) of 0.595, which is above 0.04, is suggestive that there is wide variation in the particle size; ranging from nano to micro. The high value of PDI might increase the possibility of agglomeration of the particles during solidification. This is in agreement with findings as reported in [12] where it was reported that high PDI led to adverse effects on the properties of the composite as a result of agglomeration if certain treatments are not carried out during the nano facture.
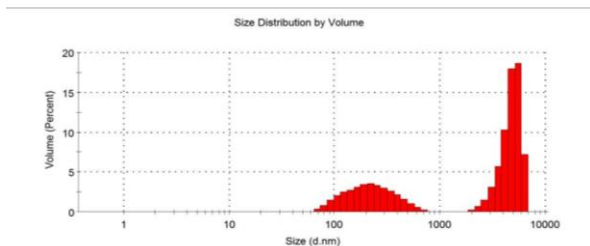
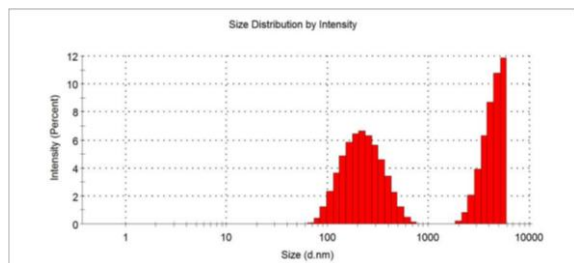Figure 2: Particle size distribution according to the volume of the particles

Figure 3: Particle size distribution according to the intensity of particles

b. X-ray diffraction (XRD) patterns of DPNSAp

The result of the X-ray diffraction carried out on the DPNSA particulate showed the presence of Quartz (SiO_2), Albite (Na Al Si_3 O_8), Muscovite (H_2 K Al_3 ($SiO_4)_3$), Orthoclase(Al_2 O_3 · K_2 O ·6 Si O_2), Chlorite (Al-Fe-SiO_2-O) and Sylvite (KCl). The highest peak noticed represented Quartz and Albite compounds with 44 and 41% respectively as shown in Figure 4. The mineralogical composition of the material, having an abundance of Quartz and Albite, suggests that the material may exhibit enhanced mechanical strength and durability when used as a reinforcement for Aluminium and its alloys. This corroborated the work of Hossam et al as reported in [13] that the

mechanical properties of Poly-Vinyl Chloride (PVC) pipes were improved by reinforcing with Doum Palm leaves particulates. Furthermore, the presence of Muscovite as shown on the Diffractograph might offer improved wear resistance as suggested in [14] where the wear resistance was improved with the percentage of Muscovite in the Al-Mg-Si-T6 alloy matrix.
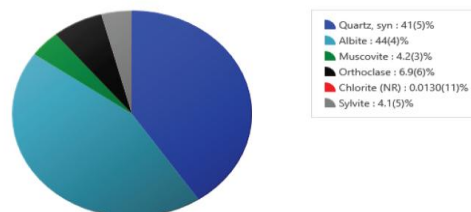

Figure 4: Pie chart showing the composition distribution of the compounds present in the DPNSAp.

c. Corrosion Test Result

This section discusses the results of the corrosion tests.

• Liner polarization of the as-cast samples

Table 1 shows the results of the LPR test carried out on the as-cast samples which were extrapolated from the Tafel curves in Figures 5.1-5.4. It can be seen that the corrosion rate decreased from 4.18 mils/year in the control sample to 1.87 mil/year in the 9% reinforced substrate. The highest corrosion rate of 9.98 mils/year was observed in the sample with 3% reinforcement. The current density also increased from $3.17x10^{-5}$ to $1.44x10^{-4}$ A/cm^2 in the Control sample and 9% reinforced substrate respectively.

Table 1: Polarization parameters for the developed Al 3.5%Cu-0.8%Mg /DPNSAp composite as-cast) in artificial seawater.

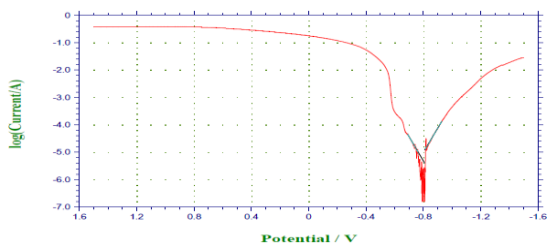| S/No	Percentage reinforcement	Cathodic slope (1/v)	Anode slope (1/v)	Polarization resistance (Ω)	Corri (A)	Ecorr	Corrosion rate (mil/year)	Corrosion rate (g/m^2.h)
1	Control	8.746	8.862	779	$3.171x10^{-5}$	-0.8	4.148	$1.671x10^{-5}$
2	3%	8.015	2.994	516	$7.650x10^{-5}$	-1.15	9.982	$4.032x10^{-5}$
3	6%	7.824	2.249	144	$2.992x10^{-4}$	-0.9	39.05	$1.577x10^{-4}$
4	9%	7.500	2.450	304	$1.436x10^{-4}$	-0.95	1.873	$7.567x10^{-5}$

Fig. 5.1: Tafel plot for the as-cast Al-3.5%Cu-0.8%Mg alloy (control) in artificial seawater.

Fig 5.2: Tafel plot for the 3% reinforced Al 3.5%Cu-0.8%Mg/DPNSAp composite in artificial seawater.
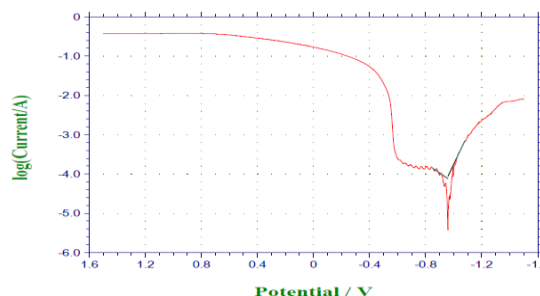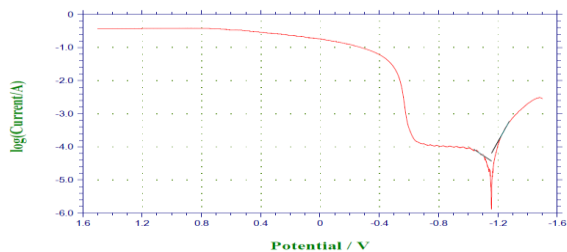

Fig 5.3: Tafel plot for the 6% reinforced Al-3.5%Cu-0.8%Mg/DPNSAp composite in artificial seawater.
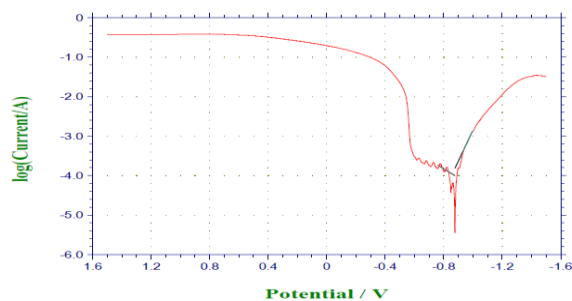

Figure 5.4: Tafel plot for the 9% reinforced Al-3.5%Cu-0.8%Mg/DPNSAp composite in artificial seawater.

• Liner polarization of the aged samples

Table 2 shows the result of the aged DPNSAp composite which was extrapolated from Figure 6.1-6.4 where it was observed that the corrosion rate initially increased at 3% reinforcement to 14.400 mil/year from 1.919 mil/year in the control sample then it further decreased to 2.305 and 1.393 mil/year in the 6 and 9% reinforced samples respectively. The cathodic and anodic slopes both decreased from 11.697 and 7.564 in the control sample to 9.532 and 2.002 in the 9% reinforced substrates respectively.

Table 2: polarization parameters for the aged Al 3.5%Cu-0.8%Mg /DPNSAp composite (aged) in artificial seawater.

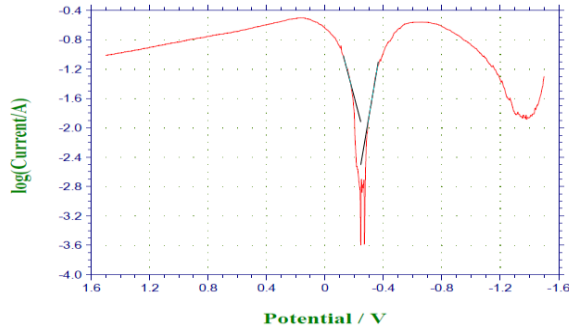| S/No	Percentage reinforcement	Cathodic slope (1/v)	Anode slope (1/v)	Polarization resistance (Ω)	Corri (A)	Ecorr	Corrosion rate (mils/year)	Corrosion rate (g/m^2.h)
1	Control	11.697	7.564	93	2.440×10^{-4}	-0.25	1.919	1.772×10^{-4}
2	3%	8.288	0.018	17	3.148×10^{-3}	-0.1	14.3	2.287×10^{-3}
3	6%	13.525	0.419	61	5.109×10^{-4}	-0.4	2.305	1.114×10^{-4}
4444	9%	9.532	2.002	123	3.067×10^{-4}	-0.6	1.393	2.227×10^{-4}

Figure 6.1: Tafel plot for the aged Al-3.5%Cu-0.8%Mg alloy (control) in artificial seawater.
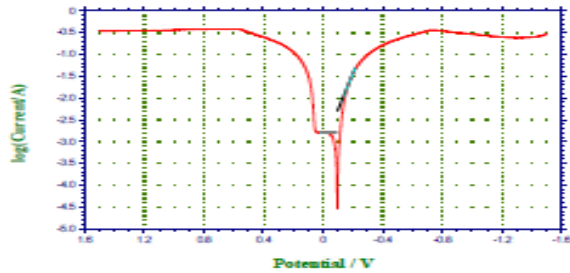

Figure 6.2: Tafel plot for the aged 3% reinforced Al-3.5%Cu-0.8%Mg/DPNSAp composite in artificial seawater.
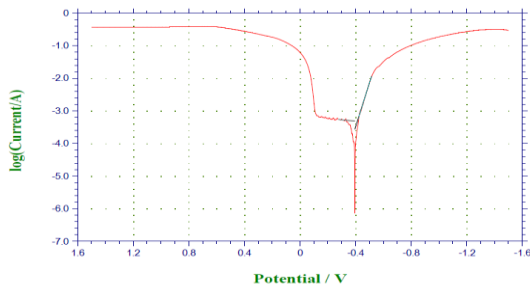

Figure 6.3: Tafel plot for the aged 6% reinforced Al 3.5%Cu-0.8%Mg/DPNSAp composite in artificial seawater.
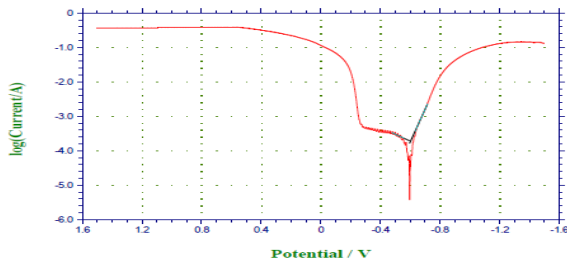

Figure 6.4: Tafel plot for the aged 9% reinforced Al 3.5%Cu-0.8%Mg/DPNSAp composite in artificial seawater.

• Influence of thermal ageing on the samples

Figure 7 compares the corrosion rates of the as-cast and aged samples where it was generally observed that the corrosion rate decreased in the aged samples which might be a result of the homogenization of the particles in the Al-Matrix by breaking up areas with particle concentration along grain boundaries as a result of agglomeration. By comparison, the values of E_{corr} for the as-cast samples are more negative than those of the ages samples, this indicates that there is a decreased tendency for the corrosion reaction to occur as the Free energy becomes more positive. This is in agreement with the research as reported in [13] where it was observed that there was a decrease in the pitting potential as a consequence of the evenly distribution of the particles leading to an increase in the volume fraction of SiC particles in the Al-Matrix.
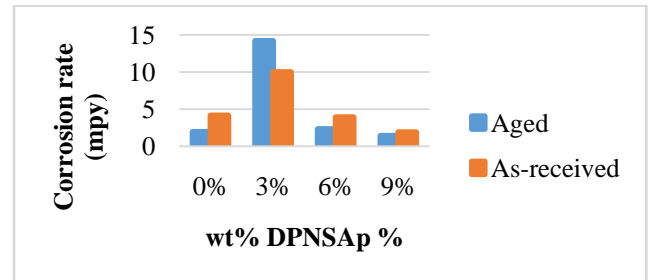

Figure 7: Corrosion rates of the as-received and aged samples obtained using linear polarization resistance (LPR).

• Scanning Electron Microscopy (SEM)

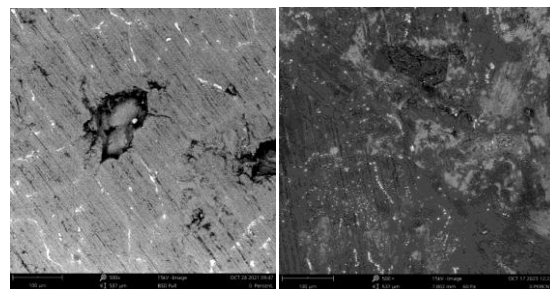Plates 1 and 2 show the morphologies of the developed samples before ageing.


(a)   (b)

Plate 1: SEM micrographs of control sample Al 3.5%Cu-0.8%Mg Alloy

Plates 1 and 2 show the micrographs of the developed samples; Plate 1 (a) shows the control sample (base

alloy) where craters and crevices were observed with A-Cu/Al-Cu-Mg intermetallics observed in the ά-Al matrix while the Plate 1 (b) shows the morphology of the aged Al-3.5%-0.8%Mg alloy where it can be observed that the Al-Cu intermetallics are distributed evenly in the matric and with fewer crates and cracks. Zakaria *et al.* [15]reported the concentration of reinforcement along the grain boundaries and the interfacial bond between the Aluminium and the SiC particles prevented the initiation and propagation of pits leading to a reduction in the corrosion rate.
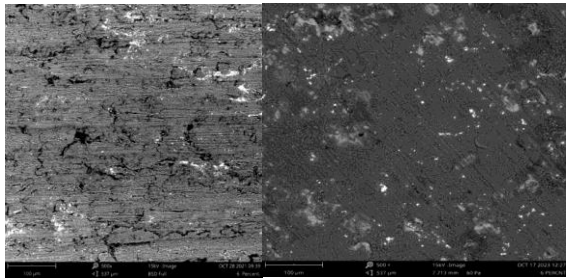
(a)   (b)

Plate 2: SEM micrograph of 6% reinforced Al 3.5%Cu-0.8%Mg/DPNSAp composite.

Plate 2 (a) shows the 6% reinforced composite with dark striations and particles of the DPNSAp agglomerating along grain boundaries with bright Al-Cu/Al-Cu-Mg intermetallic particles in the Aluminium matrix while Plate 2 (b) shows the aged and 6% reinforced composite where the agglomerated reinforcement particles observed in figure 2 (a) are not visible as a result of dispersion of the particles into the matrix during the thermal treatment.

CONCLUSION

The development, age hardening and electrochemical corrosion studies of the DPNSAp composite, after particle size analysis, XRD, LPR and SEM analysis has led to the following conclusions: The average particle size of the reinforcement was established to be 639.6nm. The morphological examination of the base alloys after corrosion revealed pits and craters with $CuAl_2$ internermetallics within the aluminium matrix, which showed localize corrosion along the grain boundaries after exposure to the artificial seawater. The reinforced particles were also seen agglomerating along the grain boundaries and cracks

in the reinforced composite. Ageing of the samples reduced the corrosion rate of the samples by 73.5% in the as-cast and aged samples and 25.7% in the controlled sample. It is therefore, recommended that as-cast sample should be allowed to aged before used in seawater environment to enhance their corrosion resistance.

REFERENCES

[1] V. S. Aigbodion and S. B. Hassan, "Effects of silicon carbide reinforcement on microstructure and properties of cast Al-Si-Fe/SiC particulate composites," *Mater. Sci. Eng. A*, vol. 447, no. 1–2, pp. 355–360, Feb. 2007, doi: 10.1016/j.msea.2006.11.030.

[2] V. S. Aigbodion, "Particulate-strengthened of Al-Si alloy/alumino-silicate composite," *Mater. Sci. Eng. A*, vol. 460–461, pp. 574–578, Jul. 2007, doi: 10.1016/j.msea.2007.01.148.

[3] N. Afzal, T. Shah, and R. Ahmad, "MICROSTRUCTURAL FEATURES AND MECHANICAL PROPERTIES," vol. 45, no. 6, pp. 684–692, 2013.

[4] B. Jegdi, "Corrosion behaviour of AA2024 aluminium alloy in different tempers in NaCl solution and with the CeCl 3 corrosion inhibitor," no. August, pp. 1–13, 2019, doi: 10.1002/maco.201911219.

[5] O. B. Umaru, M. Abdulwahab, A. Tokan, A. M. Bello, and H. A. Umar, "Effect of double thermal ageing treatment on the mechanical properties of Al-Cu-Mg/3% rice husk ash composite," *Results Phys.*, vol. 6, pp. 342–345, 2016, doi: 10.1016/j.rinp.2016.06.009.

[6] M. R. Monshi, "Synergistic Erosion and Corrosion Behavior of AA5052 Aluminum Alloy in 3 . 5 wt % NaCl Solution Under Various Impingement Angles," *J. Bio- Tribo-Corrosion*, pp. 3–9, 2015, doi: 10.1007/s40735-015-0010-3.

[7] S. A. Seth, I. S. Aji, and A. Tokan, "Dynamic Mechanical Analysis of Polypropylene Reinforced Doum Palm Shell Particles Composite," vol. 7, no. 8, pp. 645–649, 2018.

[8] P. H. Tjahjanti, W. H. Nugroho, and N. F. Ganda, "Study of Corrosion Penetration Rate on

Composite Materials EN AC-43100 (AlSi10Mg (b)) + SiC *," vol. 6, pp. 1–9, 2019.

[9] M. Gobara, A. Baraka, R. Akid, and M. Zorainy, "Corrosion protection mechanism of Ce4+/organic inhibitor for AA2024 in 3.5% NaCl," pp. 2227–2240, 2020, doi: 10.1039/c9ra09552g.

[10] M. K. Abbass, K. S. Hassan, and A. S. Alwan, "Study of Corrosion Resistance of Aluminum Alloy 6061/SiC Composites in 3.5% NaCl Solution," *Int. J. Mater. Mech. Manuf.*, vol. 3, no. 1, pp. 31–35, 2015, doi: 10.7763/ijmmm.2015.v3.161.

[11] S. B. Hassan and V. S. Aigbodion, "Effects of eggshell on the microstructures and properties of Al–Cu–Mg/eggshell particulate composites," *J. King Saud Univ. - Eng. Sci.*, vol. 27, no. 1, pp. 49–56, Jan. 2015, doi: 10.1016/j.jksues.2013.03.001.

[12] I. M. Mahbubul, "Stability and Dispersion Characterization of Nanofluid," *Prep. Charact. Prop. Appl. Nanofluid*, pp. 47–112, Jan. 2019, doi: 10.1016/B978-0-12-813245-6.00003-4.

[13] H. S. El-Beltagi, H. I. Mohamed, H. N. Yousef, and E. M. Fawzi, "Biological Activities of the Doum Palm (Hyphaene thebaica L.) Extract and Its Bioactive Components," in *Antioxidants in Foods and Its Applications*, InTech, 2018.

[14] S. Sharma, T. Nanda, and O. P. Pandey, "Effect of particle size on dry sliding wear behaviour of sillimanite reinforced aluminium matrix composites," *Ceram. Int.*, 2018, doi: 10.1016/j.ceramint.2017.09.132.

[15] H. M. Zakaria, "Microstructural and corrosion behavior of Al / SiC metal matrix composites," *Ain Shams Eng. J.*, vol. 5, no. 3, pp. 831–838, 2014, doi: 10.1016/j.asej.2014.03.003.